Structural Relaxation of Glass-Forming Polymers Based on an Equation for Configurational Entropy. 1. DSC Experiments on Polycarbonate

J. L. Gómez Ribelles* and M. Monleón Pradas

Departamento de Termodinámica Aplicada, Universidad Politécnica de Valencia, P.O. Box 22012, E-46071 Valencia, Spain

Received August 9, 1994; Revised Manuscript Received March 27, 1995[⊗]

ABSTRACT: A phenomenological model for the process of structural relaxation in glass-forming materials is discussed. The model is based on an expression for the evolution of the configurational entropy of the material when subjected to an arbitrary thermal history and contains four fitting parameters. The prediction of the model is presented in terms of heat capacity $c_p(T)$ curves, which are compared with the experimental DSC heating scans. Experimental results on polycarbonate with a broad series of thermal histories are presented, and the routine employed to fit the parameters of the model is described. The procedure permits the determination of material parameters (independent of thermal history) of the polymer: a curve of calorimetric equilibrium relaxation times as a function of temperature and a value for the width parameter of the Kohlrausch–Williams–Watts relaxation function. The possibility that the limit states of the structural relaxation process do not coincide with the states obtained from the extrapolation of the experimentally determined liquidus curve is also discussed.

1. Introduction

Structural relaxation is the term which designates the process of approach to an equilibrium state undergone by a glass held in constant environmental conditions after its formation history.[1,2] This process is revealed in the time evolution of several thermodynamical or physical variables such as specific volume or enthalpy, mechanical storage or loss moduli, dielectrical permittivity, *etc.* The kinetics of the process described in terms of functions of time and thermal history is different for different variables.[3,4] Thus it is usual to speak about "volume relaxation" or "enthalpy relaxation" to refer to the structural relaxation process as characterized by means of the evolution of the specific volume or the specific enthalpy, respectively, after a certain thermal history.[3,5–8] One of the experimental techniques most frequently used for the study of structural relaxation is differential scanning calorimetry (hereafter DSC). A sample of the amorphous, glass-forming material is subjected to a thermal history starting at a temperature T_0 higher than its glass transition temperature T_g; after successive stages involving cooling and eventually heating at controlled rates, and isothermal periods, the sample is brought to a temperature T_1 below T_g and subsequently heated from T_1 to T_0, while the specific heat capacity c_p is recorded as a function of the temperature T. This delivers useful information related to the process of structural relaxation of the sample which has taken place before and during the measuring scan itself.

In order to fully exploit this experimental information, great importance is attached to the development of mathematical models which allow the comparison of experimental $c_p(T)$ curves measured after different thermal histories with theoretical predictions. This comparison leads to the determination of values for the free parameters in the model. The models mostly used contain four parameters. These are meant to be characteristic of the material and independent of the thermal history. Thus the model should be able to reproduce the experimental results determined after any thermal history with a single set of parameters. Nevertheless, this is not the case, and it has been frequently reported that different sets of parameters are necessary to reproduce accurately the $c_p(T)$ curves measured after different thermal histories.[7,9–11] If a single set of parameters is determined from the fit to a series of thermal histories, the models usually predict $c_p(T)$ curves measured after an isothermal annealing at a temperature near T_g with peaks narrower and higher than the experimental ones.[9,12] This effect is very clear when the annealing time is long enough and the annealing temperature is on the high-temperature side of the glass transition interval, a thermal treatment which is not frequent in the literature. A similar effect can be found when $c_p(T)$ curves measured after cooling at very high and very slow rates from equilibrium are fitted simultaneously with the same set of parameters.[13] It cannot be excluded that the search routine may have some role in these difficulties.

Assumptions of two kinds are made when theories of structural relaxation are developed. In the first place, there are those concerning the very physical concept or image of the process. In this respect, both the models based on molecular theories[6,14–18] and the phenomenological models holding a macroscopic point of view[12,19–22] have been able to reproduce the most salient features of structural relaxation, even though discussion still continues on several specific questions. In the second place, both approaches are in need of more special assumptions concerning certain parameters or material functions of the models (form of the specific heat of the glass and the liquid, definition of the length of the chain segment, shape of the distribution of relaxation times, *etc.*). This second kind of supposition may have little influence on the model prediction of the $c_p(T)$ curves corresponding to different thermal histories, but can heavily affect the values of the material parameters determined from them.

Besides these assumptions, the very way in which the model equations are compared with the experimental results constitutes a third aspect of the problem which deserves a close analysis: in particular, whether or not

[⊗] Abstract published in *Advance ACS Abstracts,* July 1, 1995.

0024-9297/95/2228-5867$09.00/0

it is possible to determine characteristic material parameters and functions from this comparison.

In the present study we employ a phenomenological model and address the second and the third of these questions. In common with previous phenomenological theories, our model uses the Adams and Gibbs equation,[35] first proposed in ref 22 and exploited in ref 12, as well as a reduced time and a Kohlrausch–Williams–Watts relaxation function. We analyze the possibility of determining from a set of experimental results a set of parameters independent of the thermal history of the experimental process, and thus characteristic of the material under study, and examine the influence on the values of these parameters of the suppositions made in the equations concerning the specific configurational heat capacity. For this matter we propose an equation for the configurational entropy instead of considering the fictive temperature, as is usual in works on structural relaxation since the times of Tool. This point of view allows us to employ directly (an extension of) Adams and Gibbs' equation for the relaxation times and to avoid the normalization of the experimental $c_p(T)$ curves needed to construct the dT_f/dT curves, based on extrapolation of the liquid and glass curves of the heat capacity. As a consequence, all equations derived from the model are compatible with different expressions for the configurational heat capacity, whose influence on the values of the model parameters can be thus tested.

We check the predictions of the model against experimental results on Bisphenol A polycarbonate, a polymer which has been the subject of many experimental studies of the structural relaxation process with many different techniques.[12,23–32] In a subsequent study we compare the model with results on a family of methacrylate polymers.[33]

2. Experimental Section

Samples of Bisphenol A polycarbonate (Lexan 141/111 from General Electric Plastics) were molded at 250 °C to sheets approximately 1 mm thick for the dynamic-mechanical and dielectric experiments, or to films 0.3 mm thick for the DSC experiments. The polymer was dried *in vacuo* at 160 °C to constant weight.

Calorimetric experiments were carried out in a differential scanning calorimeter Perkin-Elmer DSC4 calibrated with standard indium and sapphire samples, and the data were collected in a TADS 3700 data station. A single 11 mg sample enclosed in an aluminum pan was used in all the measurements.

All thermal treatments were carried out in the calorimeter. They always started with an annealing at 180 °C for 10 min to erase the effects of previous thermal histories and to ensure that the polymer was in an equilibrium state. Whenever the thermal history included an isothermal annealing, the cooling rate to attain the annealing temperature T_a was 40 °C/min. After an annealing time t_a the sample was cooled again at a rate of 40 °C/min until 100 °C, the temperature selected for the start of the measuring scan, and then heated at a rate of 10 °C/min to 180 °C. Heat flux was recorded only during the heating scan, and the $c_p(T)$ curve was calculated from it. We will call hereafter a reference scan the heating scan which follows a cooling from 180 °C to 100 °C at 40 °C/min.

A series of measurements were conducted without the isothermal annealing stage, with cooling rates ranging from 1 to 40 °C/min. The heating rate was always 10 °C/min, the heating rate used for the calibration of the calorimeter.

Dynamic-mechanical experiments were performed in a Polymer Laboratories dynamic mechanical thermal analizer DMTA-II in the double cantilever mode, with a free length of 5 mm. Measurements were conducted isothermally. The temperature varied from 100 to 180 °C in steps of 5 deg.

Dielectric experiments were conducted isothermally, from 100 to 200 °C in the frequency range between 200 Hz and 100 kHz using a General Radio 1620A capacitance bridge with a Balsbaugh LD3 cell.

3. Constitutive Equation for Configurational Entropy and Model Equations

As is usual in phenomenological theories of structural relaxation, the relevant thermodynamical variables are regarded as functions of the whole thermal history experienced by the sample. We analyze here the configurational entropy S_c under this point of view. If T^t is the temperature history up to time instant t, $T(\sigma)$, $-\infty < \sigma \le t$, this fact is expressed by putting $S_c(t) = \bar{S}_c(T^t)$ (we consider here only the dependence on temperature of S_c; other variables, such as pressure, are regarded as constant, as in fact happens in DSC). $\bar{S}_c$ is a nonlinear functional of its argument, the thermal history. Whereas linear memory effects can all be represented in terms of a single model (Boltzmann's linear hereditary equation), such a universal representation does not exist for nonlinear relationships. Some additional assumptions are thus necessary to fix the form of $\bar{S}_c$. Models proposed up to now for the evolution of the properties monitored during the structural relaxation process are assumed linear in the temperature history when this last is expressed in a "reduced time" scale.[20] This is possible because the thermodynamical variables being followed are enthalpy, specific heat capacity, or specific volume, or the corresponding fictive temperatures. Since we aim here at an equation for the configurational entropy, no such assumption is allowed. We suppose instead that after a suitable rescaling of the time variable, given by a strictly increasing mapping $\xi = \hat{u}(t)$ which takes into account the changing structure of the material, $\bar{S}_c$ is expressible in the form of a "quasilinear" equation,

$$\bar{S}_c(T^t) = G(T(t)) - \int_{-\infty}^{\xi} \phi(\xi - u)\, dF(\tilde{T}(u)) \qquad (1)$$

where the integration is in the sense of Riemann–Stieltjes (with the composite function $(F \circ \tilde{T})$ being the integrating function). For any fixed T^t, in this equation $\xi = \hat{u}(t)$, and $\tilde{T}(u)$, $-\infty < u \le \xi$, is the history of temperature expressed in the new time scale, *i.e.*, $\tilde{T}(u) = T(\tilde{t}(u))$, where $\tilde{t}(u) = t$ denotes the inverse mapping of $\hat{u}(t)$. In (1), G, F, ϕ, and $\hat{u}$ are functions characterizing the material. Their number can be reduced and their form established with the help of some natural additional hypotheses.

First of all, we should like ϕ to behave as a normalized relaxation function and thus impose that it decrease monotonically and

$$\lim_{u \to \infty} \phi(u) = 0 \quad \text{and} \quad \lim_{u \to 0} \phi(u) = 1 \qquad (2)$$

Further, we want the configurational entropy $S_c(t)$ to have its equilibrium value $S_c^{eq}(T^*)$ at any temperature T^* if the thermal history of the sample has been the constant history $T(\sigma) = T^*$ for all $-\infty < \sigma \le t$: $\bar{S}_c(T^*) = S_c^{eq}(T^*)$. Substitution of this condition in (1) gives $G = S_c^{eq}$. For the equilibrium configurational entropy we assume

$$S_c^{eq}(T) = \int_{T_2}^{T} \frac{\Delta c_p(\theta)}{\theta}\, d\theta \qquad (3)$$

where $\Delta c_p(T)$ is the specific configurational heat capacity at temperature T. Thus a temperature T_2, Gibbs and DiMarzio's transition temperature,[34] is assumed to exist for which S_c^{eq} vanishes, see ref 35.

Consider now the temperature-jump history $T(\sigma) = T_a + (T_b - T_a)\, h(\sigma)$, $-\infty < \sigma \le t$, where h denotes Heaviside's unit step function and T_a and T_b are any two arbitrary temperatures. Equation 1 yields $S_c(\sigma) = S_c^{eq}(T_a)$ for $\sigma < 0$ and

$$S_c(\sigma) = S_c^{eq}(T_b) - \phi(\hat{u}(\sigma))\,(F(T_b) - F(T_a)) \qquad (4)$$

for $\sigma \ge 0$. In contrast to what happens to other thermodynamical variables such as specific volume or enthalpy, which may experience instantaneous changes at temperature jumps, configurational entropy is continuous through any such a jump: in the case being considered, $\lim_{\sigma\to 0+} S_c(\sigma) = \lim_{\sigma\to 0-} S_c(\sigma) = S_c^{eq}(T_a)$. Taking limits in (4) and recalling (2), we get $S_c^{eq}(T_a) - S_c^{eq}(T_b) = F(T_a) - F(T_b)$, valid for any two T_a and T_b. From here, $dS_c^{eq}(T)/dT = dF(T)/dT$. Thus, summing up, these hypothesis lead to a reduced form of (1)

$$\tilde{S}_c(T^t) = S_c^{eq}(T(t)) - \int_{-\infty}^{\hat{u}(t)} \phi(\hat{u}(t) - u)\, dS_c^{eq}(T(\tilde{t}(u))) \qquad (5)$$

When compared with linear constitutive equations, which are always expressible in the form of Boltzmann's hereditary integral law $\int_{-\infty}^{t} M(t - \sigma)\, dT(\sigma)$, we notice that nonlinearity in (5) has two sources: first, past temperatures influence the present value of configurational entropy through S_c^{eq} weighted by ϕ; second, as shall be later seen, $\hat{u}(t)$ (and thus also $\tilde{t}(u)$) depends on $S_c(t)$ itself.

For any temperature-jump thermal history, $T(t) = T_1 + (T^* - T_1)\, h(t)$, we have, from (5), $S_c(t) = S_c^{eq}(T_1)$ for $t < 0$, and

$$S_c(t) = S_c^{eq}(T^*) - \phi(\hat{u}(t))\,(S_c^{eq}(T^*) - S_c^{eq}(T_1)) \qquad (6)$$

for $t \ge 0$. Thus we get

$$\phi(\hat{u}(t)) = \frac{S_c(t) - S_c^{eq}(T^*)}{S_c^{eq}(T_1) - S_c^{eq}(T^*)} \qquad (7)$$

This equation justifies the consideration of ϕ as a relaxation function. For a multiple-step temperature history, $T(t) = T_0 + \sum_{i=1}^{n}(T_i - T_{i-1})\, h(t - t_{i-1})$ (with $t_0 = 0$),

$$S_c(t) = S_c^{eq}(T(t)) - \sum_{i=1}^{n}(S_c^{eq}(T_i) - S_c^{eq}(T_{i-1}))\, \phi(\hat{u}(t) - \hat{u}(t_{i-1})) \qquad (8)$$

$$= S_c^{eq}(T(t)) - \sum_{i=1}^{n}\left(\int_{T_{i-1}}^{T_i} \frac{\Delta c_p(T)}{T}\, dT\right) \phi(\hat{u}(t) - \hat{u}(t_{i-1})) \qquad (9)$$

and for a constant-rate history, when $T(t) = T_0 + qt\, h(t)$ is substituted in (5) we have

$$S_c(t) = S_c^{eq}(T(t)) - q\int_0^{\hat{u}(t)} \phi(\hat{u}(t) - u)\frac{\Delta c_p(\tilde{T}(u))}{\tilde{T}(u)}\, d\tilde{t}(u) \qquad (10)$$

Nonexponentiality, one of the most clearly recognized experimental features of structural relaxation,[20,21,36] is accounted for in our model by assuming a form of ϕ given by a Kohlrausch–Williams–Watts-type[37] formula: for $0 \le u < \infty$

$$\phi(u) = \exp(-u^{\beta}) \qquad (11)$$

It is also an experimental fact that master curves can be constructed for the relaxation process out of curves obtained at different temperatures by a shifting procedure[20] (conceptualization of the structural relaxation process as a sum of individual exponential processes characterized by relaxation times τ_i which all have the same temperature dependence is a way to give this empirical fact some foundation[21]). This feature is incorporated through the definition of a "reduced time" scale; see ref 20. For simplicity in the definition of this time scale we consider only thermal histories $T(\sigma)$, $-\infty < \sigma \le t$, which were constant up to time instant $\sigma = 0$; *i.e.*, we consider only temperature histories T^t of the form $T(\sigma) = T_0 + f(\sigma)\, h(\sigma)$, where T_0 is any temperature and $f(\sigma)$ is any function. The time scale transformation is then assumed to be given by

$$\hat{u}(t) = \int_0^t \frac{d\sigma}{\hat{\tau}(\sigma)} \qquad (12)$$

where, as in ref 22, we take in this equation $\hat{\tau}(\sigma) = \tau(S_c(\sigma), T(\sigma))$ and

$$\tau(S_c, T) = A \exp\left(\frac{B}{S_c T}\right) \qquad (13)$$

Equation 13 is an extension of Adam and Gibbs' expression for the equilibrium relaxation times to states out of equilibrium: when the configurational entropy S_c in it has the equilibrium value $S_c^{eq}(T)$, we have

$$\tau(S_c^{eq}(T), T) = A \exp\left(\frac{B}{S_c^{eq}(T)T}\right) = \tau^{eq}(T) \qquad (14)$$

A is here a pre-exponential constant; the parameter B in Adam and Gibbs' theory is

$$B = \frac{s_c \Delta\mu}{k} \qquad (15)$$

where s_c means the configurational entropy of the smallest cooperatively rearranging region, $\Delta\mu$ is the free energy barrier hindering configurational rearrangement per mole of molecules or chain segments, and k is Boltzmann's constant.

The mapping $\hat{u}$ defined by (12) is strictly increasing and thus has an inverse mapping, $\tilde{t}(u)$. Their derivatives obey $\tilde{t}'(u) = 1/\hat{u}'(t)$ when $u = \hat{u}(t)$. From (12), $\hat{u}'(t) = 1/\hat{\tau}(t)$, and thus $\tilde{t}'(u) = \hat{\tau}(t) = \hat{\tau}(\tilde{t}(u)) = \tilde{\tau}(u)$, a result which can be substituted in (10) to give

$$S_c(t) = S_c^{eq}(T(t)) - q\int_0^{\hat{u}(t)} \phi(\hat{u}(t) - u)\frac{\Delta c_p(\tilde{T}(u))}{\tilde{T}(u)}\tilde{\tau}(u)\, du \qquad (16)$$

Notice that ϕ in (5) has reduced time as its argument. A "relaxation function" $\hat{\phi}(t)$ with actual time as argument can be defined through $\hat{\phi}(t) = \phi(\hat{u}(t))$; for each t, the value of $\hat{\phi}$ depends on the thermal history experienced by the material.

When the assumptions (11)−(13) are introduced in (5), a constitutive equation for configurational entropy out of equilibrium results which has, besides the function $\Delta c_p(T)$, four adjustable parameters: A, B, T_2, and β. Three of them, A, B, and T_2, together with $\Delta c_p(T)$ define the dependence of the equilibrium relaxation times on temperature, (14); β can be interpreted as a width parameter of a distribution of relaxation times.

Given a set of values for the four model parameters, the $\Delta c_p(T)$ curve has a key role in the behavior predicted by eqs 5, 9, and 16. In principle, the expression for $\Delta c_p(T)$ should be considered an experimental datum: the difference between the specific heat capacity curves determined for the equilibrium liquid and for the glassy states, $c_{pl}(T)$ and $c_{pg}(T)$, respectively. The difficulty is that both functions cannot be determined simultaneously in any temperature interval, and so the calculation of $\Delta c_p(T)$ is always based on an extrapolation. Usually, linear expressions for $c_{pl}(T)$ and $c_{pg}(T)$ are assumed, and as a consequence, $\Delta c_p(T)$ is a linear function of T too,[38]

$$\Delta c_p(T) = A_1 + A_2 T \tag{17}$$

usually with negative A_2 values in a way such that Δc_p vanishes at a certain temperature above T_g. The equation

$$\Delta c_p(T) = \frac{\Delta c_p(T_g) T_g}{T} \tag{18}$$

has also been frequently used (as in Hodge's AGV model[12]) because it simplifies the calculations. In this expression Δc_p is also a decreasing function of temperature, but it does not vanish at any finite value of temperature.

Some additional uncertain points are related to the determination of the specific configurational heat capacity. One difficulty lies in the identification of $c_{pg}(T)$ with the experimental values of $c_p(T)$ measured for temperatures below the glass transition. DSC measurements are highly reproducible if experimental conditions remain unchanged. This is the case when several consecutive heating scans are conducted on the same sample with different thermal histories but changing neither the position of the sample pan in the apparatus' holder nor the position of the its cover. In this way it becomes possible to determine the temperature interval, below the glass transition, in which the experimental $c_p(T)$ curve is independent of the thermal history. In the present work, reproducible heat capacity values independent of the thermal history have been found in the temperature range between 110 and 130 °C in the above mentioned experimental conditions. From these values the expression for the $c_{pg}(T)$ curve has been calculated. Nevertheless, in this temperature range a significant conformational mobility still remains. This is revealed by the fact that isothermal annealing at temperatures within this interval, or even at temperatures as low as 80 °C (results not shown), leads to significant changes in the $c_p(T)$ curve which appear at higher temperatures. It is reasonable to keep in mind the possibility that the accepted c_{pg} values still contain a certain component due to configurational degrees of freedom. Experiments in a very wide temperature range would help to be conclusive on this point, looking for changes in the curvature of $c_{pg}(T)$ that could indicate the onset of the conformational motions. Unfortunately, the accuracy of DSC measurements in a too wide temperature interval probably would not be high enough due to the curvature of the baseline.

Another difficulty arises if some part of the heat capacity increment Δc_p in the glass transition would reside in internal degrees of freedom. This possibility was pointed out by Goldstein.[39] According to him, when the temperature rises past T_g, changes in vibration frequencies, anharmonicity, or changes in the number of molecular groups participating in motions which are detected as secondary relaxations would be responsible for this. For polycarbonate there are reports of a substantial influence on the strength of the secondary dielectric or dynamic-mechanical relaxations of the configurational state in the glass attained after different thermal histories starting above T_g.[31,32] The strength of such relaxation peaks, and thus the number of molecular groups participating in them, decreases as the structural relaxation process progresses, *i.e.*, as the number of available configurations or the configurational entropy or the fictive temperature decreases. Conversely, when the temperature rises through the glass transition and a greater number of configurations is available to the polymer segments, the polymer groups that were not able to participate in the secondary relaxations in the glassy state may become free for these motions, contributing to the vibrational specific heat capacity with new degrees of freedom.

The above arguments make difficult a definitive choice of the expression for the dependence of Δc_p with temperature, whether to take (17) and (18) or even an equation independent of temperature. As a consequence, it seems interesting to keep open the possibility of studying the effect of the different expressions for $\Delta c_p(T)$ on the model predictions. This possibility is enhanced by our model.

Equation 5 together with (11)−(13) is an integral equation for $S_c(t)$ which must be solved numerically. In this work cooling and heating stages in the thermal histories were replaced by a series of 1-deg temperature jumps followed by isothermal stages with a duration calculated to result in the same overall rate of temperature change as in the actual experiments. The configurational entropy was calculated at time instants t_k with (9), and the relaxation time at those time instants is then calculated using (13). This value of the relaxation time is used to calculate the reduced time in the subsequent time instant t_{k+1}, according to (12). After each temperature jump the reduced time was evaluated in time instants $t_k = 0.001 \cdot 2^k$ seconds, with integer k.

Comparison of the experimental results with the model calculations requires that they be expressed in terms of $c_p(T)$ curves. Owing to the inherent irreversibility of the structural relaxation process, there is no straightforward relationship between the configurational entropy and $c_p(T)$. However, it is true that

$$c_p(T) - c_{pg}(T) = \frac{\partial H_c}{\partial T}$$

where H_c is the specific configurational enthalpy. For the dependence of H_c upon the thermal history an analogous derivation to that of S_c is assumed, which leads to the equation, analogous to (9),

$$H_c(t) = H_c^{eq}(T(t)) - \sum_{i=1}^{n} \left(\int_{T_{i-1}}^{T_i} \Delta c_p(T)\, dT \right) \phi_H(\hat{u}(t) - \hat{u}(t_{i-1}))$$

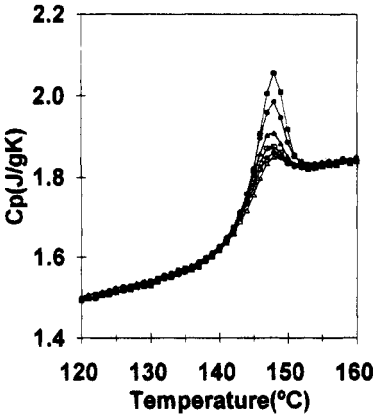

Figure 1. Temperature dependence of the specific heat capacity c_p measured in heating scans after cooling from 180 °C at different rates: (△) 40 °C/min; (○) 20 °C/min; (□) 10 °C/min; (▲) 5 °C/min; (●) 2 °C/min; (■) 1 °C/min.

for a stepped temperature history. The assumption made here in order to determine H_c is that the relaxation function ϕ_H coincides with the entropy's relaxation function ϕ; *i.e.*, it is assumed that the relaxation times for enthalpy and entropy are the same, and consequently, they are also the same for the Gibbs free energy.

The set of four parameters of the model was determined by a simultaneous least-squares fit to a set of five experimental $c_p(T)$ curves obtained after five significantly different thermal histories (those shown in Figure 2 and defined in the caption to this figure). The correlation between the four parameters has been amply reported for phenomenological models as those of Narayanaswamy–Moynihan or Scherer–Hodge[7,9,10,12,13,40-43] and is also found in the one proposed in the present work. Mainly, a correlation is found between B and T_2 (see below). To avoid this problem, the parameter B was fixed while the other three were adjusted. The fitting procedure was conducted for different values of B. The Nedler and Mead[44] search routine was employed.

4. Results

The set of $c_p(T)$ curves measured after thermal histories without an isothermal annealing stage is shown in Figure 1. The main feature of these experiments is the peak which appears at a temperature of 148 °C nearly independent of the cooling rate. The height of the peak decreases as the cooling rate increases, but even at 40 °C/min, in the reference scan, a small peak shows up.

From the curves is Figure 1 it is possible to calculate the intersection point of the specific enthalpy lines corresponding to the liquid and glassy states, which coincides with the fictive temperature in the glass, T_f. The calculation was performed according to the equation (see ref 45)

$$\int_{T_f}^{T^*} (c_{pl}(T') - c_{pg}(T'))\,dT' = \int_{T_1}^{T^*} (c_p(T') - c_{pg}(T'))\,dT' \quad (19)$$

where $c_p(T)$ is the specific heat capacity measured in the experimental scan, c_{pl} and c_{pg} are the specific heat capacities of the liquid and the glass, respectively, T_1 is the lowest temperature of the experiment, and T^* is a temperature high enough in the liquid state. The values of T_f calculated from (19) are shown in Table 1 as a function of the cooling rate. The difference between these values and the temperatures of the intersection of the entropy lines in the liquid and the glassy states is only ±0.3 deg.

Table 1. Fictive Temperature in the Glassy State after Cooling from 180 °C at Different Cooling Rates

Cooling rate (°C/min)	T_f (K)	Cooling rate (°C/min)	T_f (K)
1	410.7	10	413.4
2	412.0	20	413.9
5	412.7	40	415.0

In this work we take the value of T_f measured in the reference scan, 142 °C, as the glass transition temperature, T_g, of the sample. This value is slightly higher than the onset of the transition, $T_{g,onset}$ which in our reference scan is 140 °C and slightly lower than the midpoint T_g, determined from the midpoint of the c_p increment in the transition: 143 °C. The three values of the different usual definitions of T_g are close to each other in this polymer because of the narrow range in which the transition takes place.

The $c_p(T)$ curves measured after thermal treatments with isothermal annealing at 100, 120, and 140 °C are shown in Figure 2, together with the predictions of the model. The annealing time was about 1000 min at 120 and 140 °C. The annealing time was longer at 100 °C because this temperature is quite far from T_g; shorter annealing times do not lead to a peak additional to that already showing up in the reference scan but result only in a small shoulder on the curve at temperatures below this peak. The peak in the low-temperature side of the glass transition characteristic of the annealing at low temperatures which appears in other polymers[9,10,12,43,46-50] (see also ref 33) does not appear in polycarbonate with the annealing temperatures selected in this work.

A series of experiments with different annealing times at 120 °C were conducted. The $c_p(T)$ curves measured are represented in Figure 3a. From them the increment of enthalpy in the isothermal stage $\Delta h(T,t) = h(T,0) - h(T,t)$ (with T, t the annealing temperature and time, respectively) was determined. The calculation procedure was the one described in refs 9 and 51. The results are shown in Figure 4.

Master curves for the dynamic-mechanical storage modulus E' and loss modulus E'' could be drawn by making use of time–temperature superposition,[52] taking 150 °C as the reference temperature (Figure 5). The horizontal shifts (in the logarithm of frequency axis), $\log a_T$, needed to build the master curves are shown in Table 2. Small shifts in the logarithms of E' and E'' (vertical axis), $\log a_v$, were also necessary (see Table 2). This form of presentation of our data has to be considered just as an estimate of the shape of the relaxation curves at 150 °C in a broad range of frequencies, between 10^{-6} and 10^4 Hz, not available experimentally. The maximum of E'' at this temperature appears at 6.8 Hz (angular frequency $\omega_m = 42.7\ s^{-1}$).

The procedure followed with the dielectric results was similar to that just described. Master curves for ϵ' and ϵ'' (real and imaginary parts of the complex dielectric permittivity) were obtained by superposition on the 170.7 °C isotherm (Figure 6). Vertical shifts were not necessary in this case. Horizontal shifts are shown in Table 3. The maximum in ϵ'' in the 170.7 °C isotherm appears at 1.17×10^4 Hz (angular frequency $\omega_m = 7.33 \times 10^4\ s^{-1}$).

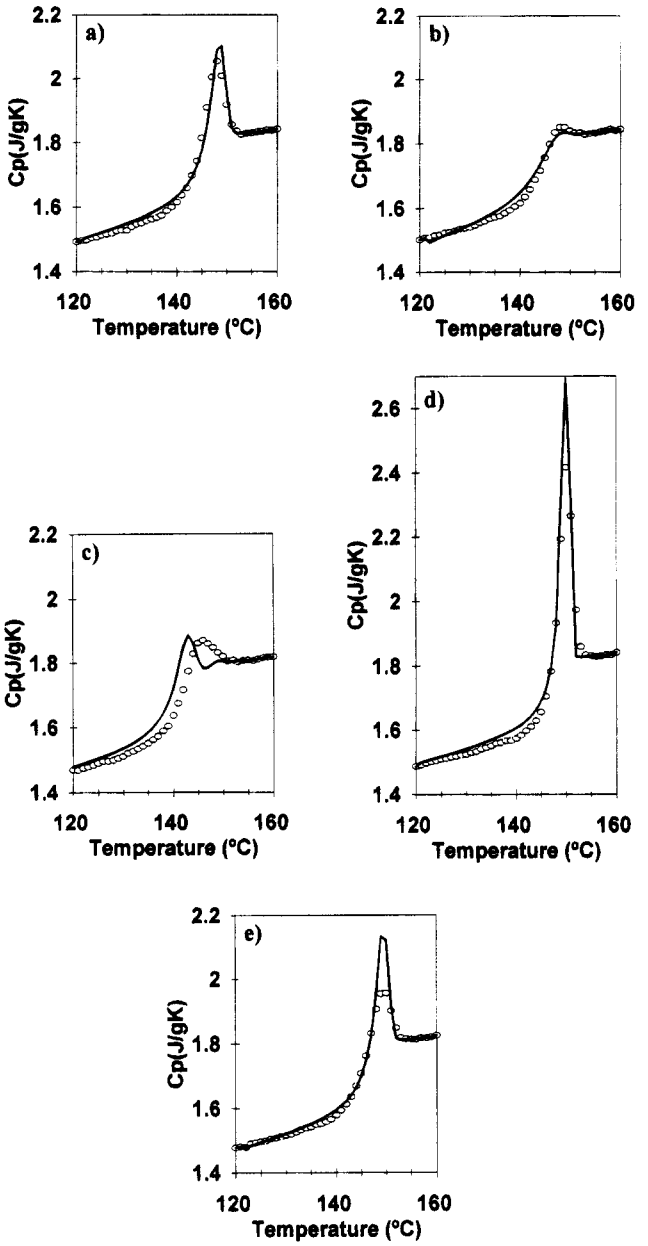

Figure 2. Experimental $c_p(T)$ curves measured after cooling at 1 °C/min (a) and 40 °C/min (b) and after thermal histories that include an isothermal annealing at 100 °C for 4440 min (c), 120 °C for 1010 min (d), and 140 °C for 1005 min (e). The solid line represents the prediction of the model with Δc_p following eq 20, $B = 1250$ J/g, and the rest of the parameters shown in Table 4. The circles correspond to the experimental values.

5. Discussion

Application of the Model with a Linear Expression for $\Delta c_p(T)$. The parameters in (17) were determined with a least-squares fit of the experimental $c_p(T)$ values to a linear equation in the liquid (between 160 and 180 °C) and glassy (between 110 and 130 °C) temperature ranges. The expression accepted for the configurational heat capacity was taken as the average of those found for the complete set of experimental results,

$$\Delta c_p = 0.8505 - 0.001521T \; J/(g\,K) \qquad (20)$$

Figure 2 shows the fit obtained keeping $B = 1250$ J/g fixed. The values of A, T_2, and β obtained with the search routine are shown in Table 4. The curves predicted by the model are close to the experimental ones, a remarkable feature in them being the fact that the peak in the $c_p(T)$ curve measured after an annealing at 140 °C is higher in the model than in the experiment. This fact has also been found in other polymers.[33] The peak in the curve measured after annealing at 100 °C appears in the model slightly shifted toward lower temperatures. The shape of the curve after thermal treatments which involve annealing at low temperatures is quite different in different polymers. In fact, the fit in the methacrylate polymers,[33] which show a prepeak in the $c_p(T)$ curve after this treatment, is quite better than in polycarbonate.

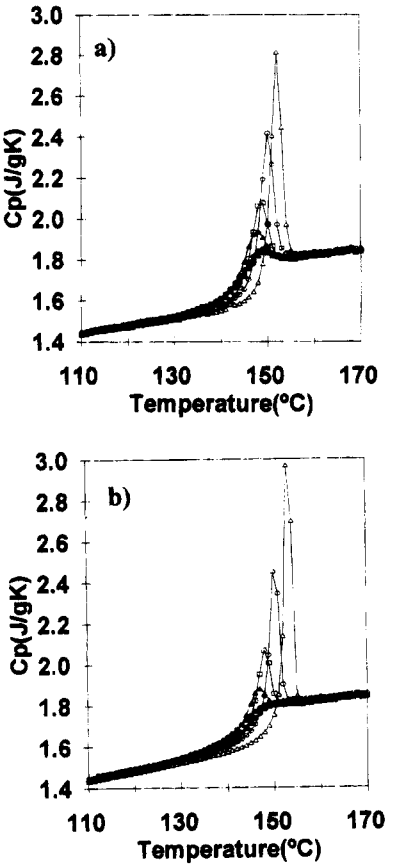

Figure 3. Specific heat capacity after annealing at 120 °C for different temperatures: (■) 10 min; (●) 30 min; (▲) 115 min; (□) 300 min; (○) 1005 min; (△) 4090 min; experimental values (a) and model predictions (b).

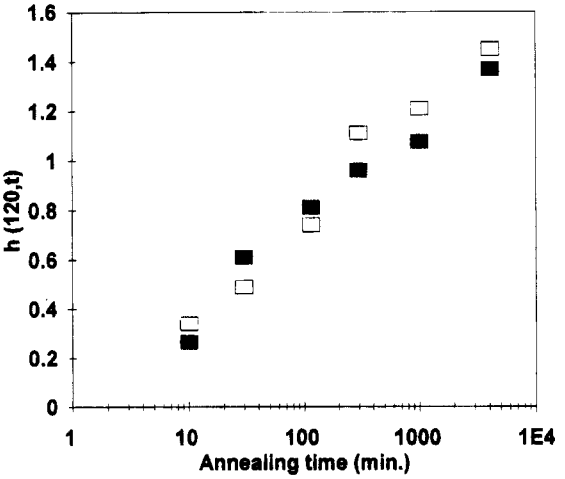

Figure 4. Enthalpy increment during isothermal annealing at 120 °C as a function of annealing time: (■) experimental results, (□) model calculations.

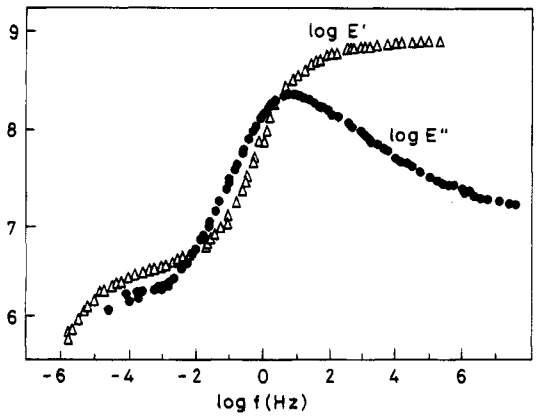

Figure 5. Master curves of the real and imaginary parts of the dynamic-mechanical modulus, E' and E'', constructed on the 150 °C isotherm.

Table 2. Horizontal and Vertical Shift Factors, log a_T and log a_v, Respectively, Needed To Superpose each E' and E'' Isotherm on the 150 °C One To Draw the Master Curve of Figure 4[a]

T (°C)	log a_T	log a_v	log τ_M (s)	T (°C)	log a_T	log a_v	log τ_M (s)
165	−3.13	−0.07	−4.93	145	1.39	0.05	−0.41
160	−2.26	−0.06	−4.06	140	2.9	0.1	1.10
155	−1.28	−0.04	−3.08	135	4.88	0.13	3.08
150	0	0	−1.8	130	6.22	0.14	4.42

[a] The parameter τ_M of the KWW equation is also included.

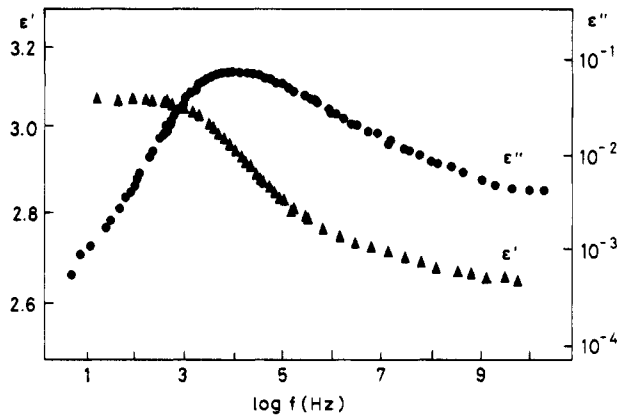

Figure 6. Master curves for the real and imaginary parts of the dielectric permittivity, ϵ' and ϵ'', constructed on the 170.7 °C isotherm.

Table 3. Horizontal Shift Factors log a_T Needed To Superpose Each ϵ' and ϵ'' Isotherm on the 170.7 °C One To Draw the Master Curve of Figure 5[a]

T (°C)	log a_T	log τ_D (s)	T (°C)	log a_T	log τ_D (s)
194.5	−2.23	−7.26	170.7	0	−5.03
189.9	−1.91	−6.94	167.5	0.45	−4.58
186.1	−1.66	−6.69	163.3	1.264	−3.77
182.5	−1.36	−6.39	158.0	2.22	−2.81
179.1	−1.02	−6.05	153.3	3.42	−1.62
176.6	−0.76	−5.79	148.2	5.27	0.24
173.6	−0.42	−5.45			

[a] The parameter τ_D of the KWW equation is also included.

The values obtained for the model parameters are significantly different for the different values of B selected, as shown in Table 4. Nevertheless, for any of the thermal histories the curves predicted by the model with the different sets of parameters corresponding to values of B ranging between 1000 and 2000 J/g are nearly coincident. The only exception is the scan corresponding to an annealing at 100 °C. Here the height of the peak in the theoretical curve increases with increasing B values (see Figure 7). Thus, there exist different sets of four parameters which lead to nearly identical predictions for the $c_p(T)$ curves. It must be pointed out that, in this respect, the model here employed and the Narayanaswami–Moynihan or the Scherer–Hodge models exhibit the same features. In fact, much attention has been devoted to the independent determination of one of the model parameters. Instead of exploting an *a priori* argument to determine the value of the parameter B, in the present study we prefer to start out by making calculations with different values of this parameter, thus arriving at the results of Table 4, to later analyze the arguments that can be adduced to choose one value. Below we consider some of the arguments employed to eliminate this overdetermination of the phenomenological models. These arguments rely on the assumed universality of certain features of the glass transition such as the relationship between T_2 and T_g, or on the experimental determination of the temperature dependence of the equilibrium relaxation times in an interval around T_g using experiments after different cooling rates. Though these arguments can be of help in reducing the uncertainty of the numerical determination of the parameter values, the procedure here employed shows that none of them suffices for an unambiguous and independent determination of one of the parameters. The reason for the model's overdetermination lies probably in the fact that the analytical dependence of the relaxation times on temperature and structure contains three parameters, which may be too many. Equations based on free volume theories also contain three parameters.[2,8,53] To our knowledge, none of the equations proposed for out-of-equilibrium states contain fewer parameters.

Table 4. Model Parameters Found by the Search Routine for Each Value of B and Each Expression for $\Delta c_p(T)$

B (J/g)	β	$S_c^{eq}(T_g)$ [J/(g K)]	ln A (s)	T_2 (K)	$T_g - T_2$ (K)	T_g/T_2	$[\partial/\partial(1/T)]$ ln $\tau^{eq}(T_g)$ (kK)
			$\Delta c_p(T)$ as in Eq 20				
1000	0.43	0.0415	−52.7	355.1	59.9	1.17	151.6
1250	0.45	0.0481	−57.9	347.7	67.3	1.19	144.2
1500	0.46	0.545	−61.6	340.9	74.1	1.22	138.2
1750	0.48	0.0612	−64.3	334.3	80.7	1.24	131.1
2000	0.49	0.0672	−67.1	328.6	86.4	1.26	126.9
			Δc_p Independent of Temperature				
1250	0.42	0.0539	−51.14	338.6	76.4	1.23	
			Δc_p as in Eq 18				
1250	0.44	0.0494	−56.2	338.7	76.3	1.23	
			Δc_p as in Figure 10, with $\Delta = 0.12$				
1250	0.48		−57.3	347.6	67.4	1.19	

The correlation among the parameters of the model appears quite clearly. When B increases, lower values of T_2 and of ln A are obtained. These three parameters determine the curve of equilibrium relaxation times. Figure 8 shows the τ^{eq} curves determined from the different sets of parameters of Table 4. There is an outstanding coincidence between these curves, at least in the time interval comprised between 10^{-5} and 10^3 s. The equilibrium relaxation time is 100 s when the temperature is equal to T_g for all the sets of parameters. The differences between the different curves start being significant at low temperatures. This may explain why only the c_p curves measured after isothermal annealing at 100 °C seem to be affected by the value of parameter B fixed in the search routine. In any event, the equilibrium relaxation times are sensitive to the values

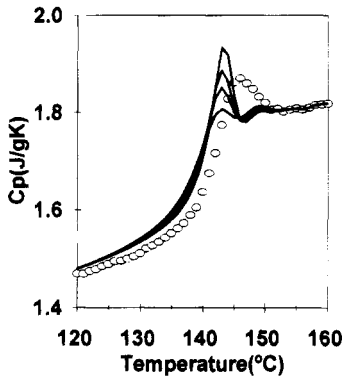

Figure 7. $c_p(T)$ measured after a thermal history that includes an isotherml annealing at 100 °C for 4440 min. Model calculations with B = 1000, 1250, 1500, and 2000 J/g (and the rest of the parameters according to Table 4) are shown in solid lines. The peak appearing in c_p at approximately 142 °C decreases for increasing values of B; this identifies the different curves. The experimental results are represented by open circles.

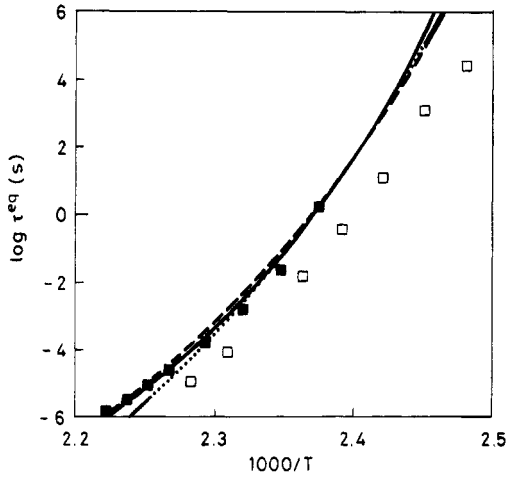

Figure 8. Equilibrium relaxation times determined by the model for different values of B (see text): (—) B = 1000 J/g; (· — ·) B = 1500 J/g; (- - -) B = 2000 J/g. The relaxation times obtained from dynamic-mechanical (□) and dielectric (■) relaxation studies are also shown.

of the set of parameters only in a time interval clearly 1 order of magnitude greater than the experimental times.

There is also some correlation between the value of B and the one found by the search routine for β, which varies from 0.43 to 0.49 when B varies from 1000 to 2000 J/g.

As a consequence of all this, it is possible to conclude that the experimental results on polycarbonate define a single curve of equilibrium relaxation times, which can be accurately determined between 130 and 180 °C, but the analytical expression for this curve is compatible, within the accuracy of this method, with different sets of three parameters. This, in practice, leads to a high uncertainty in the determination of each one of them. The only experimental datum which would allow the determination of B, and consequently fix the rest of parameters, would be the response after long annealing periods at low temperatures. Concerning the thermal histories in the present work, this argument supports a choice of a value of B close to 1250 J/g. But a more extensive study on different polymers would be necessary to check this hypothesis.

Support from other types of experiments or theoretical arguments seems necessary for an independent determination of one of the parameters. This would be the case if one of these parameters were "universal", at least for some class of amorphous material. One of the parameters that could play this role is the configurational entropy at the glass transition temperature, $S_c^{eq}(T_g)$. From (3)

$$S_c^{eq}(T_g) = \int_{T_2}^{T_g} \frac{\Delta c_p(\theta)}{\theta} d\theta \qquad (21)$$

$S_c^{eq}(T_g)$ values calculated for the different sets of parameters are displayed in Table 4. A universal value for this parameter would mean that the glass transition occurs when the number of conformations available for the molecule segments or material units attains a certain critical value, an argument parallel to that of free volume theories that claim the existence of a universal value for the fractional free volume at T_g.[52] Obviously, to be conclusive in this point it is necessary to compare systematically this value for different materials with similar behaviors in the glass transition (for instance, in the case of the materials in this work, for the substances called fragile by Angell[54]) and to settle the ambiguity in the definition of the term *glass transition temperature*.

Another possibility in this regard refers to the value of the parameter T_2. For polymers behaving as fragile according to the classification of Angell one may expect values of T_g/T_2 close to 1.1 ÷ 1.3, the order of magnitude of the values reported by Adam and Gibbs[35] from viscoelastic results. In polycarbonate, the glass transition is quite narrow, and probabily because of this the values of T_g/T_2 fall within this interval for all the sets of parameters of Table 4. The difference $T_g - T_2$ varies from 60 to 87 °C. The more reasonable values, taking into account what is found in viscoelastic or dielectric measurements, are those close to 50 °C, which correspond to the lowest values of B. Nevertheless the determination of T_2 from viscoelastic or dielectric experiments is not free from difficulties. The uncertainty in the determination of T_2 made by fitting the ln τ *vs* T curves to the Williams–Landel–Ferry (WLF)[55] or Vogel–Fulcher–Tammann–Hesse (VFTH) equations[56-58] is high, and the calculation is frequently done by assuming universal values of the parameters c_1 and c_2 of the WLF equation.[52]

Another source of information that has been employed for an independent determination of one of the parameters in a phenomenological model is data for T_g values obtained after cooling from equilibrium at different cooling rates. This allows the determination of the slope of the ln τ^{eq} *vs* $1/T$ curve:[45]

$$\frac{\partial \ln \tau^{eq}}{\partial(1/T)} = \frac{\partial \ln q}{\partial(1/T_f)} \qquad (22)$$

The experimental values of Table 1 allow us to calculate

$$\frac{\partial \ln \tau^{eq}}{\partial(1/T)} = 154 \pm 11 \text{ kK} \qquad (23)$$

The value of this slope calculated from the model as a function of B and $S_c^{eq}(T_g)$ is

$$\frac{\partial \ln \tau^{eq}}{\partial(1/T)} = \frac{B}{S_c^{eq}(T_g)}\left(1 + \frac{T}{S_c^{eq}(T_g)}\frac{\partial S_c^{eq}}{\partial T}\right) \qquad (24)$$

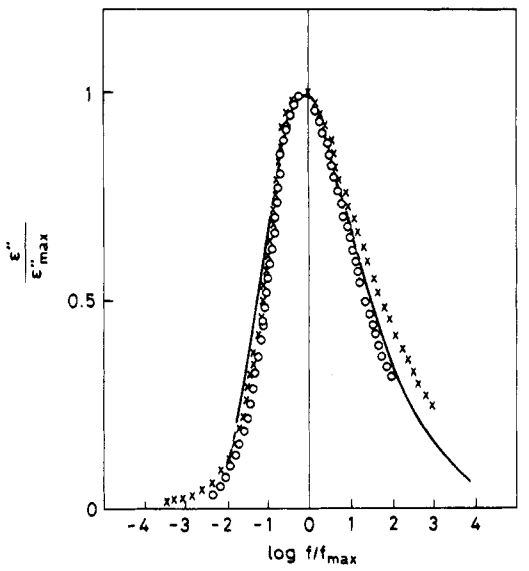

Figure 9. Master curves for the normalized main dynamic-mechanical (E''/E''_{max}) (×) and dielectric ($\epsilon''/\epsilon''_{max}$) (○) relaxations and the calculated one with the KWW equation with $\beta = 0.4$ (solid line).

The values calculated with the different sets of parameters are shown in Table 4. None of them is very far from the experimental value, but again the fits carried out with the values of B around 1250 J/g are the best.

The equilibrium relaxation times determined by DSC can be compared with those determined from dynamic-mechanical and dielectrical measurements through the temperature dependence of the quantity τ in the Kohlrausch–Williams–Watts equation:[37]

$$\phi(t) = \exp(-(t/\tau)^{\beta}) \qquad (25)$$

The master curves in Figures 5 and 6 were fitted to the KWW model. It is assumed that there is no significant change of the value of the β parameter with temperature. The fitting procedure was the one proposed by Williams, Watts, Dev, and North.[59] A value of $\beta_{dm} = 0.40$ was found both for the dynamic-mechanical and dielectric main relaxations. The model curve is represented in Figure 9 together with the normalized experimental results. The experimental E'' data are higher than those predicted by the model in the high-frequency interval, probably due to the overlapping of a secondary relaxation that appears around 1 Hz at 100 °C.[31,60] The values of the parameter τ in the KWW equation, called here τ_M for the dynamic-mechanical relaxation and τ_D for the dielectric relaxation, were determined as functions of temperature by taking into account the position of the maximum in the master curve and the horizontal shift factors needed to build the master curve. Thus, in the dynamic-mechanical E'' isotherm at 150 °C the maximum appears at an angular frequency of 42.7 s^{-1}. Since for $\beta = 0.4$ the KWW equation predicts a maximum in E'' for $\omega\tau = 0.68$,[59] one can calculate τ_M at 150 °C and use the shift factor a_T to calculate the values corresponding to different temperatures. The data are included in Table 2 and represented in Figure 8. The same procedure has been followed to calculate the dielectric relaxation times (Table 3 and Figure 8). The values of τ_M are shorter than the corresponding calorimetric ones for the same temperature, in good agreement with what found by other authors with different procedures.[4,61,62] By contrast, τ_D values sensibly agree with calorimetric values.

The value of the parameter β calculated from the fit of the model to the DSC experimental results correlates with the remaining parameters. The values obtained with the lowest values of B, 1000 or 1250 J/g, are the closest to the ones determined by dynamic-mechanical or dielectric techniques.

The enthalpy increment during the isothermal annealing at 120 °C has been calculated from the model $c_p(T)$ curves with $B = 1250$ J/g and the corresponding values for the rest of parameters given in Table 4, following the same procedure as in the calculation from the experimental result. The model values agree sensibly with the experimental ones at all annealing times (Figure 4). This shows the good performance of the model in thermal histories different from the ones used in the least-squares fit.

Influence of the Expression for $\Delta c_p(T)$ on the Model Calculations. Limit States of the Structural Relaxation Process. The model was fitted to the experimental results with a constant value for Δc_p calculated from (20) at the temperature of 120 °C. This assumption means that some part of the measured c_p at temperatures below the glass transition has a configurational origin. Since the overall fit obtained is very similar to that found with (20) and shown in Figure 2, no additional figure is included. Nevertheless, the parameters take quite different values. The set of parameters found by the search routine with $B = 1250$ J/g and constant Δc_p is included in Table 4. The same behavior is met when (18) is the one used. The set of parameters for $B = 1250$ J/g is also shown in Table 4. The influence of the $\Delta c_p(T)$ expression is greatest on T_2, with differences of up to 12 K among the values corresponding to the different equations.

The overall accuracy of the fit allows us to consider significant the fact that the peak appearing in $c_p(T)$ after annealings at high temperatures is greater in the model prediction than in the experimental results. Works on enthalpy relaxation in amorphous polymers have reported that the extrapolation of the experimental values of $\Delta h(T,t)$ to long times leads to limiting values considerably lower than the theoretically determined ones[5,51,63,64] (a significant exception to this is constituted by ref 23; in it, heat capacity increments in the glass transition of polycarbonate seem to be compatible with the limiting values of the enthalpy loss during the isothermal annealing at temperatures very close to T_g). This raises doubts concerning the usual identification of the limit state of the isothermal structural relaxation process at a temperature T with the state obtained at T from the extrapolation of the equilibrium, or liquidus, curve measured at temperatures above T_g. This argument would support the hypothesis of a metastable state, intermediate between those of equilibrium liquid and glass, as the limiting condition of the material in the structural relaxation process, which accordingly would be unable to reach the equilibrium state. The reason for this could lie in a collapse of the configurational rearrangements when the number of conformations available for the molecules or polymer segments would attain a certain limit value higher than the one corresponding to equilibrium. Topological constraints such as entanglements, present in polymers but not in inorganic glasses, could explain why structural relaxation in polymers would exhibit this distinctive feature.[64]

The relationship of this question to the existence of nonconfigurational contributions to $\Delta c_p(T)$ is not clear.

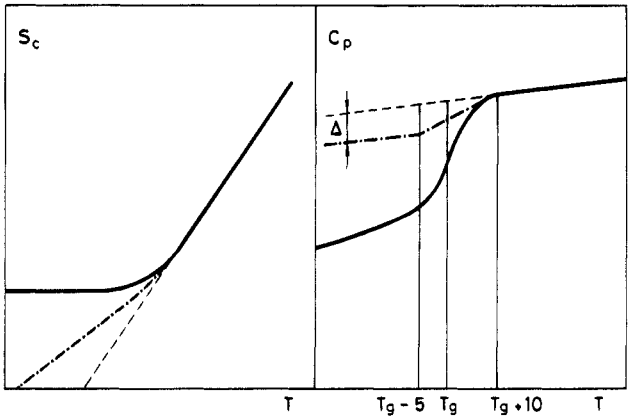

Figure 10. (a, Left) Sketch of the configurational entropy corresponding to the liquid state (dashed line), to an experimental cooling scan at a finite cooling rate (solid line) and to the metastable state line, possible limit of the structural relaxation process (dash-dot line). (b, Right) $c_p(T)$ lines corresponding to the three cases described in a).

Even when a part of the difference between the excess entropy of the liquid and the glass, and consequently, a part of the difference between the entropy in a given glassy state and the one of the equilibrium state at the same temperature, is of vibrational origin, probably both vibrational and configurational contributions relax simultaneously. The experiments of Chang, Bestul, and Horman[65-68] support this idea. They found in different noncrystalline materials that the difference in entropy between two glassy states at the same temperature formed through different thermal histories is temperature-dependent below T_g and only a part of it remains at 0 K. The vanished entropy difference would be of vibrational origin according to Goldstein.[39]

Our model equations can be used to check whether the predicted curves under this hypotehsis are closer to experiment than those previously analyzed. The sketch of Figure 10a shows the assumed shape for the curve of metastable states in the temperature interval of the glass transition, a shape similar to that of an experimental cooling at a finite rate, but with a different change of slope. Figure 10b represents the assumption here made regarding the $c_{pl}(T)$ behavior of the limit states to be introduced in the model equations. Simply, we assume that the behavior of the eventual transition from liquid to the metastable limit states is analogous to that from the liquid to the glassy states. Per force, any hypothesis regarding these limit states of the structural relaxation introduces new parameters into the model, which, in principle, is not desirable. Our purpose here is, nonetheless, to show how the calculations based on limit states such as those in Figure 10 do allow indeed predictions of $c_p(T)$ curves closer to experiment. Keeping B fixed at 1250 J/g several values for Δ were tried. The best choice led to Δ = 0.12, somewhat over 0.5 of the vlaue of $\Delta c_p(T_g)$; the remaining parameters are given in Table 4. The calculated $c_p(T)$ curves corresponding to the thermal histories employed in the fitting routine are shown on Figure 11. The height of the peak after the isothermal stage at 140 °C is well reproduced, and more remarkably, also the peak corresponding to the thermal treatment at 100 °C does show up at the correct temperature. As an additional verification Figure 3b shows the predicted behavior after several isothermal dwell times at 120 °C; with the exception of the 1005 min treatment, these temperature histories were not employed in the fitting routine. The

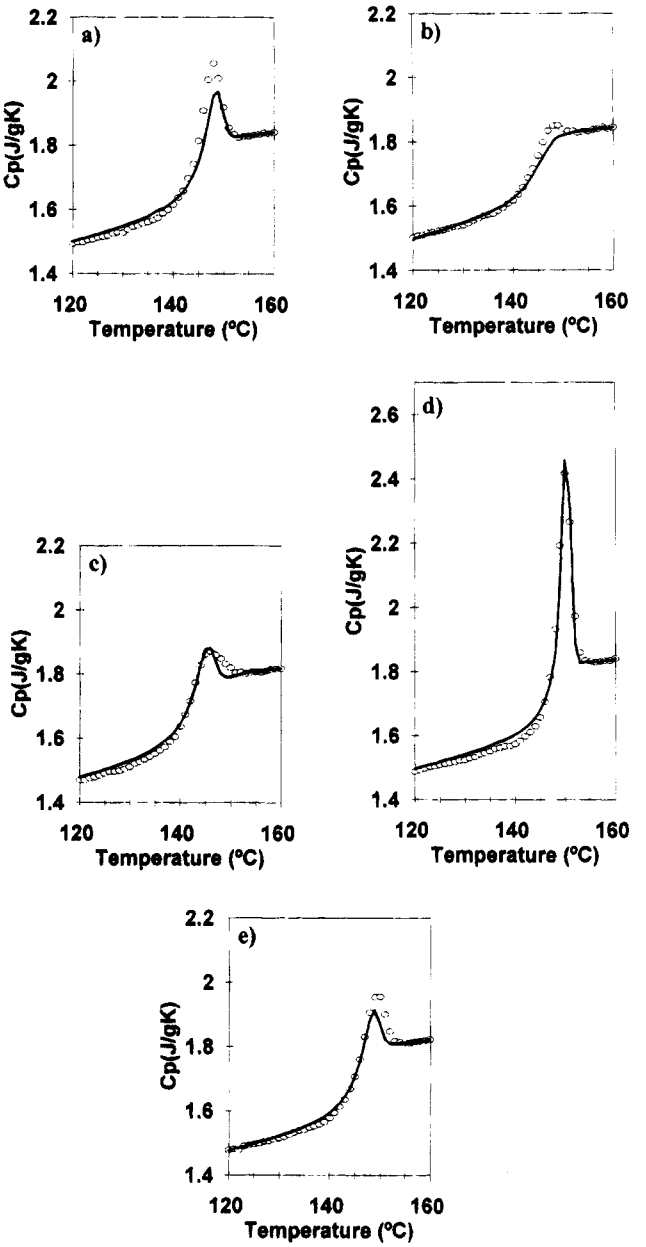

Figure 11. Model calculation with $\Delta c_p(T)$ according to the sketch of figure 10, B = 1250 J/g, and the rest of the parameters according to Table 4. The thermal histories of each curve have been defined in Figure 2.

shape of the predicted c_p curves, position and height of the maxima included, is very close to the experimental one.

6. Concluding Remarks

This paper was intended to examine the application of the phenomenological theories of structural relaxation based on the use of the Adam and Gibbs equation relating the structural relaxation times with the configurational entropy, in the direction of the works of Scherer and Hodge. Some significant ways in which our procedure departs from these authors are the following.

(1) The model equations are expressed in terms of the configurational entropy instead of fictive temperature. On the one hand this makes it easier to analyze the influence of the assumptions regarding Δc_p on the model predictions.

(2) On the other hand it allows us to consider hypothetical limit states of the structural relaxation

process of the glass which differ from the states obtained by extrapolating the equilibrium liquidus curve. The analysis on polycarbonate here presented suggests that these limit states could be significantly separated from the equilibrium ones. In order to be conclusive on this point a wider experimental study on more types of glass-forming materials would be necessary. To our knowledge, this question had not been up to now undertaken by the previous phenomenological studies: in the models based on the fictive temperature concept it is simply assumed that when time goes to infinity, at any temperature T, the fictive temperature T_f goes to its equilibrium value, T.

(3) The fitting routine of the model parameters is consistent with their consideration as material functions, that is, independent from the thermal history considered. An overdetermination of the model has been found, in the sense that more than one set of four (or five) parameter values lead to the same curve of c_p-(T). However, the method permits the determination, within reasonable error bounds, of two unique material parameters for polycarbonate which can be obtained from DSC results: a curve of relaxation times in equilibrium and the width parameter β of the KWW equation. A unique determination of the parameters B, T_2, and $\ln A$ necessitates complementary experimental techniques, or perhaps calorimetric experiments with thermal histories significantly different from those here employed. It was possible to compare the DSC results with dynamic-mechanical and dielectrical results obtained on the same material.

Acknowledgment. This work was supported by the Spanish CICYT through project MAT 91-0578.

References and Notes

(1) Davies, R. O.; Jones, G. O. *Adv. Phys.* **1953**, *2*, 370.
(2) Hodge, I. M. *J. Non-Cryst. Solids* **1994**, *169*, 211.
(3) Adachi, K.; Kotaka, T. *Polym. J.* **1982**, *14*, 959.
(4) Pérez, J.; Cavaille, J. Y.; Díaz Calleja, R.; Gómez Ribelles, J. L.; Monleón Pradas, M.; Ribes Greus, A. *Makromol. Chem.* **1991**, *192*, 2141.
(5) Cowie, J. M. G.; Ferguson, R. *Macromolecules* **1989**, *22*, 2307.
(6) Pérez, J. *Polymer* **1988**, *29*, 483.
(7) Tribone, J. J.; O'Reilly, J. M.; Greener, J. *Macromolecules* **1986**, *19*, 1732.
(8) Mijovic, J.; Nicolais, L.; D'Amore, A.; Kenny, J. M. *Polym. Eng. Sci.* **1994**, *34*, 381.
(9) Gómez Ribelles, J. L.; Ribes Greus, A.; Díaz Calleja, R. *Polymer* **1990**, *31*, 223.
(10) Romero Colomer, F.; Gómez Ribelles, J. L. *Polymer* **1989**, *30*, 849.
(11) Prest, W. M.; Roberts, F. J., Jr.; Hodge, I. M. *Proc. NATAS Conf., 12th* **1980**, 119–123.
(12) Hodge, I. M. *Macromolecules* **1987**, *20*, 2897.
(13) Moynihan, C. T.; Crichton, S. N.; Opalka, S. M. *J. Non-Cryst. Solids* **1991**, *131–133*, 420.
(14) Robertson, R. E. *Ann. N.Y. Acad. Sci.* **1981**, *371*, 21.
(15) Robertson, R. E.; Simha, R.; Curro, J. G. *Macromolecules* **1984**, *17*, 911.
(16) Ngai, K. L. *Comments Solid State Phys.* **1979**, *9*, 127.
(17) Chow, T. S. *Polym. Eng. Sci.* **1984**, *24*, 1079.
(18) Chow, T. S. *Adv. Polym. Sci.* **1992**, *103*, 149.
(19) Moynihan, C. T.; Macedo, P. B.; Montrose, C. J.; Gupta, P. K.; DeBolt, M. A.; Dill, J. F.; Dom, B. E.; Drake, P. W.;Easteal, A. J.; Elterman, P. B.; Moeller, R. P.; Sasabe, H. *Ann. N.Y. Acad. Sci.* **1976**, *279*, 15.
(20) Narayanaswamy, O. S. *J. Am. Ceram. Soc.* **1971**, *54*, 491.
(21) Kovacs, A. J.; Aklonis, J. J.; Hutchinson, J. M.; Ramos, A. R. *J. Polym. Sci., Polym. Phys.* **1979**, *17*, 1097.
(22) Scherer, G. W. *J. Am. Ceram. Soc.* **1984**, *67*, 504.
(23) Bauwens-Crowet, C.; Bauwens, J. C. *Polymer* **1986**, *27*, 709.
(24) Bauwens-Crowet, C.; Bauwens, J. C. *Polymer* **1987**, *28*, 1863.
(25) Hill, A. J.; Heater, K. J.; Agrawal, C. M. *J. Polym. Sci., Polym. Phys.* **1990**, *28*, 387.
(26) Ricco, T.; Smith, T. L. *J. Polym. Sci., Polym. Phys.* **1990**, *28*, 513.
(27) Guerdoux, L.; Merchal, E. *Polymer* **1981**, *22*, 1199.
(28) Geurdoux, L.; Duckett, R. A.; Forelich, D. *Polymer* **1984**, *25*, 1392.
(29) Liu, L. B.; Yee, A. F.; Gidley, D. W. *J. Polym. Sci., Polym. Phys.* **1992**, *30*, 221.
(30) Pixa, R.; Goett, C.; Froelich, D. *Polym. Bull.* **1985**, *14*, 53.
(31) Díaz Calleja, R.; Gómez Ribelles, J. L. In *Developments in Plastics Technology-4*, Whelan, A., Goff, J. P., Eds.; Elsevier-Applied Science: London, 1989.
(32) Pathmanathan, K.; Cavaillé, J. Y.; Johari, G. P. *J. Polym. Sci., Polym. Phys.* **1989**, *27*, 1519.
(33) Gómez Ribelles, J. L.; Monleón Pradas, M.; Más Estellés, J.; Vidaurre Garayo, A.; Romero Colomer, F.; Meseguer Dueñas, J. M. *Macromolecules* **1995**, *28*.
(34) Gibbs, J. H.; DiMarzio, E. A. *J. Chem. Phys.* **1958**, *28*, 373.
(35) Adam, G.; Gibbs, J. H. *J. Chem. Phys.* **1965**, *43*, 139.
(36) Kovacs, A. J. *Fortschr. Hochpolym.-Forsch.* **1963**, *3*, 394.
(37) Williams, G.; Watts, D. C. *Trans. Faraday Soc.* **1970**, *66*, 80.
(38) Mathot, V. B. F. *Polymer* **1984**, *25*, 579.
(39) Goldstein, M. *J. Chem. Phys.* **1976**, *64*, 4767.
(40) Hodge, I. M.; Huvard, G. S. *Macromolecules* **1983**, *16*, 371.
(41) Hodge, I. M. *J. Non-Cryst. Solids* **1991**, *131–131*, 435.
(42) Más Estellés, J.; Gómez Ribelles, J. L.; Monleón Pradas, M. *Rev. Port. Hemorreol.* **1990**, *4* (Suppl. 1/Pt. A), 13.
(43) Hodge, I. M.; Berens, A. R. *Macromolecules* **1982**, *15*, 762.
(44) Nedler, J. A.; Mead, R. *Comput. J.* **1965**, *7*, 308.
(45) Moynihan, C. T.; Easteal, A. J.; DeBolt, M. A.; Tucker, J. *J. Am. Ceram. Soc.* **1976**, *59*, 12.
(46) Berens, A. R.; Hodge, I. M. *Macromolecules* **1982**, *15*, 756.
(47) Más Estellés, J.; Gómez Ribelles, J. L.; Monleón Pradas, M. *Polymer* **1993**, *34*, 3837.
(48) Ruddy, M.; Hutchinson, J. M. *Polym. Commun.* **1988**, *29*, 132.
(49) Montserrat Ribas, S. *Prog. Colloid Polym. Sci.* **1992**, *87*, 78.
(50) Montserrat Ribas, S. *J. Polym. Sci., Polym. Phys.* **1994**, *32*, 509.
(51) Gómez Ribelles, J. L.; Díaz Calleja, R.; Ferguson, R.; Cowie, J. M. G. *Polymer* **1987**, *28*, 2262.
(52) Ferry, J. D. *Viscoelastic Properties of Polymers*; Wiley: New York, 1970.
(53) Matsuoka, S.; Williams, G.; Johnson, G. E.; Anderson, E. W.; Furukawa, T. *Macromolecules* **1985**, *18*, 2652.
(54) Angell, C. A. *J. Non-Cryst. Solids* **1991**, *131–133*, 3.
(55) Williams, M L.; Landel, R. F.; Ferry, J. D. *J. Am. Chem. Soc.* **1955**, *77*, 3701.
(56) Vogel, H. *Phys. Z.* **1921**, *22*, 645.
(57) Fulcher, G. A. *J. Am. Ceram. Soc.* **1925**, *8*, 339.
(58) Tamman, G.; Hesse, W. *Z. Anorg. Allg. Chem.* **1926**, *156*, 245.
(59) Williams, G.; Watts, D. C.; Dev, S.; North, A. M. *Trans. Faraday Soc.* **1971**, *67*, 1323.
(60) Jho, J. Y.; Yee, A. F. *Macromolecules* **1991**, *24*, 1905.
(61) Moynihan, C. T.; Lesikar, A. V. *Ann. N.Y. Acad. Sci.* **1981**, *371*, 151.
(62) Sasabe, H.; Moynihan, C. T. *J. Polym. Sci.* **1978**, *16*, 1667.
(63) Cowie, J. M. G.; Ferguson, R. *Polym. Commun.* **1986**, *27*, 251.
(64) Cowie, J. M. G.; Ferguson, R. *Polymer* **1993**, *34*, 2135.
(65) Chang, S. S.; Horman, J. A.; Bestul, A. B. *J. Res. Natl. Bur. Stand., Sect. A* **1967**, *71*, 293.
(66) Chang, S. S.; Bestul, A. B. *J. Res. Natl. Bur. Stand., Sect. A* **1971**, *75*, 113.
(67) Chang, S. S.; Bestul, A. B. *J. Chem. Phys.* **1972**, *56*, 503.
(68) Chang, S. S.; Bestul, A. B. *J. Chem. Thermodyn.* **1974**, *6*, 325.

MA946331B